

# Scanning Microscopy

---

Volume 1990  
Number 4 *Fundamental Electron and Ion Beam  
Interactions with Solids for Microscopy,  
Microanalysis, and Microlithography*

---

Article 13

1990

## Electron Beam Nano-Etching in Oxides, Fluorides, Metals and Semiconductors

C. J. Humphreys  
*University of Liverpool, United Kingdom*


T. J. Bullough  
*University of Liverpool, United Kingdom*

R. W. Devenish  
*University of Liverpool, United Kingdom*

D. M. Maher  
*AT&T Bell Laboratories, New Jersey*

P. S. Turner  
*Griffith University, Australia*

Follow this and additional works at: <https://digitalcommons.usu.edu/microscopy>

 Part of the [Biology Commons](#)

---

### Recommended Citation

Humphreys, C. J.; Bullough, T. J.; Devenish, R. W.; Maher, D. M.; and Turner, P. S. (1990) "Electron Beam Nano-Etching in Oxides, Fluorides, Metals and Semiconductors," *Scanning Microscopy*. Vol. 1990 : No. 4 , Article 13.

Available at: <https://digitalcommons.usu.edu/microscopy/vol1990/iss4/13>

This Article is brought to you for free and open access by the Western Dairy Center at DigitalCommons@USU. It has been accepted for inclusion in Scanning Microscopy by an authorized administrator of DigitalCommons@USU. For more information, please contact [digitalcommons@usu.edu](mailto:digitalcommons@usu.edu).



ELECTRON BEAM NANO-ETCHING IN OXIDES, FLUORIDES, METALS AND SEMICONDUCTORS

C.J. Humphreys\*, T.J. Bullough, R.W. Devenish, D.M. Maher<sup>1</sup> and P.S. Turner<sup>2</sup>

Department of Materials Science and Engineering, University of Liverpool,  
P.O. Box 147, Liverpool L69 3BX, U.K.

<sup>1</sup>AT&T Bell Laboratories, 600 Mountain Avenue, Murray Hill, NJ 07974, USA

<sup>2</sup>Division of Science and Technology, Griffith University, Nathan, QLD 4111, Australia

Abstract

Etching, lithography, hole formation, surface restructuring and external machining can all be performed on a nanometre scale using an intense electron beam. Results are presented for a range of different materials which demonstrate the variety of mechanisms by which electron beam nano-etching can occur. For example, in crystalline  $\beta$ -alumina hole formation occurs by surface indentations growing inwards to join up and form a nanometre diameter hole. In amorphous alumina, on the other hand, hole formation is from the inside-out: oxygen gas bubbles form under the electron beam, coalesce, and burst to leave a well defined nanometre diameter hole. In MgO and Si, holes develop from the electron exit surface: whereas in Al voids form along the irradiated volume, leading eventually to the development of a hole at the electron entrance surface. The potential of electron beam nano-etching to lithography and information storage is demonstrated by showing that the entire contents of the Encyclopaedia Britannica can be written on a pinhead.

Key Words: electron beam lithography, nano-etching, lithography, electron stimulated desorption, magnesium oxide, aluminium oxide, aluminium, silicon, information storage, nanotechnology.

\*Address for Correspondence:  
Colin J. Humphreys,  
Department of Materials Science and Metallurgy,  
University of Cambridge,  
Pembroke Street,  
Cambridge, CB2 3QZ, U.K.

Telephone Number: 44-223-334457 (FAX: 334437)

Introduction

If a high current density electron beam, of nanometre scale diameter and of energy typically 100 keV, is incident upon various materials, then nanometre and sub-nanometre scale surface and volume structures (e.g. indentations, holes and lines) can be produced. It is also possible to cut a specimen to a desired shape with nanometre precision and to plane surfaces to be atomically smooth. We have called this process by the acronym SCRIBE (Sub-nanometre Cutting and Ruling by an Intense Beam of Electrons) (Humphreys *et al.*, 1985), and we propose in this paper the general term 'electron beam nano-etching' to describe the indenting, hole drilling, cutting and surface structuring which can all be performed on a nanometre scale.

It is clear that a variety of possible mechanisms exist for electron beam nano-etching, and that different mechanisms dominate in different materials. In a thin slice of sodium  $\beta$ -alumina (typically 500 Å thick) we have shown that hole formation starts by indentations forming at both surfaces: the indentations then grow inwards to form a complete hole (Mochel *et al.*, 1983). In amorphous alumina, on the other hand, we have shown that the hole formation is not from the outside-in, but from the inside-out: an oxygen gas bubble forms in the irradiated volume which then bursts through capping layers at the surfaces to form a nanometre diameter hole (Berger *et al.*, 1987). Amorphous fluorides behave similarly. Recent work on MgO cubes shows that a crystallographic indentation forms initially at both surfaces and the indentation at the electron-exit surface then propagates through the crystal to the electron-entrance surface forming a hole bounded by {100} (Turner *et al.*, submitted for publication). On the other hand, holes in metallic Al etch mainly from the electron-entrance surface through to the electron-exit surface, a highly unexpected result (Bullough *et al.*, 1990a, b). Semiconductors (e.g. Si, InP) can also be etched by 100 keV electron beams of high intensity.

In this paper we discuss the electron beam-specimen interactions for the materials mentioned above, giving results and discussing mechanisms. We also consider some applications, particularly to nanolithography and information storage. It may be of major significance that the electron beam etching discussed in this paper is a direct process, requiring no subsequent chemical development, unlike conventional electron beam lithography using organic resists. It may also be important that many materials which etch directly are inorganic and hence are compatible with UHV molecular-beam epitaxial growth.

The first demonstration of electron beam etching on a fine scale was due to Broers *et al.* (1978) who used the high current density from a LaB<sub>6</sub> filament to form 5 nm diameter

holes in NaCl. Using a field emission gun (FEG), Isaacson and Muray (1981) drilled 1.5 nm diameter holes in NaCl. The first permanent etching on a nanometre scale (holes etched in NaCl are not permanent due to attack of the NaCl by atmospheric water vapour) was performed by Mochel *et al* (1983a,b) in the ceramic material sodium  $\beta$ -alumina, again using a FEG. Devenish *et al* (1988, 1989) have recently shown that holes may be etched in sodium  $\beta$ -alumina using a standard thermionic electron source. The characteristics of electron beam etching in sodium  $\beta$ -alumina will be described first, and then the very different characteristics of etching in other materials, such as MgO will be considered. Possible mechanisms will be discussed.

#### Nano-etching in crystalline $\beta$ -alumina

Nanometre and sub-nanometre holes and lines can be directly etched in a range of crystalline  $\beta$ -aluminas (Li  $\beta$ -Al<sub>2</sub>O<sub>3</sub>, Na  $\beta$ -Al<sub>2</sub>O<sub>3</sub>, K  $\beta$ -Al<sub>2</sub>O<sub>3</sub>, Na  $\beta$ "Al<sub>2</sub>O<sub>3</sub>, Ag  $\beta$ "Al<sub>2</sub>O<sub>3</sub>, Pb  $\beta$ "-Al<sub>2</sub>O<sub>3</sub>) (Mochel *et al*, 1983a and b). There appears to be a threshold current density effect: using 100 keV incident electrons, a current density of at least  $10^7$  A m<sup>-2</sup> is required to etch holes in  $\beta$ -alumina. This is easily achieved using a FEG (Mochel *et al*, 1983a and b), and may also be achieved using a conventional thermionic source (Devenish *et al*, 1988 and 1989).

Holes can be etched through about 1000 Å of  $\beta$ -alumina in typically a few seconds, using 100 keV electrons from a FEG. Measurements of transmitted current against time during electron irradiation indicate a uniform hole growth rate of typically  $250$  Å s<sup>-1</sup> (Mochel *et al*, 1983a). Studies of partially drilled holes show that indentations form at both electron-entrance and exit surfaces, and these indentations then elongate to join up and form a hole through the specimen (Mochel *et al*, 1983b). Holes can be cut at lower threshold current densities using incident electron energies as low as 40 keV (the lowest energy tried (Mochel *et al*, 1983a)), indicating that direct displacement damage is unlikely to be the primary mechanism involved. Electron energy loss spectroscopy (EELS) performed during the hole etching process indicates that the highly mobile Na<sup>+</sup> ions in Na  $\beta$  Al<sub>2</sub>O<sub>3</sub> (or the Ag<sup>+</sup> ions in Ag  $\beta$  Al<sub>2</sub>O<sub>3</sub>, etc) move out of the electron irradiated area extremely rapidly, presumably because this area becomes positively charged owing to ionisation by the incident beam. EELS reveals that oxygen is being lost continuously and the Al:O ratio increases continuously. For example, initially the Al:O ratio is about 0.7, as expected. During drilling this ratio increases to 1.7 and higher (Berger *et al*, 1987). Energy filtered images taken after a complete hole has been formed and using the 15 eV Al plasmon loss exhibit a sheath of Al around the hole (Berger *et al*, 1987). 20 Å diameter holes cut through 1000 Å or 2000 Å thick materials have rather straight even sides, and exhibit no evidence of beam broadening: variations in hole diameter along its length are on a  $\pm 2$  Å scale, which corresponds to surface roughness on an atomic scale (Mochel *et al*, 1983b). Holes and patterns of lines cut in the  $\beta$ -alumina materials are stable to the atmosphere (Mochel *et al*, 1983b).

Specimens in good thermal contact with a conductor may be drilled, hence these high melting point  $\beta$ -alumina ceramic materials cannot be melting. For a 10 Å diameter electron probe, heat flow calculations indicate that the temperature difference between the region of the specimen under the centre of the probe and the region at the edge of the probe, about 5 Å away, is only a few degrees. If the specimen is thermally insulated, then the whole specimen may heat up and melt under electron irradiation, but even then the temperature difference between the region under the centre and under the periphery of a 10 Å probe would be only a few degrees. The well defined holes observed cannot be due to local specimen melting (Humphreys *et al*, 1985), although the radial

temperature gradient can be extremely high.

The evidence presented above suggests that holes in  $\beta$ -alumina are produced by material being removed atom plane by atom plane from both surfaces, with oxygen being desorbed following ionisation by the incident beam, and aluminium migrating to the sides of the hole (Humphreys *et al*, 1985). This is consistent with the uniform rate of hole etching observed, the ease with which relatively low energy electrons can cut holes, the oxygen loss during etching observed in EELS, and the sheath of Al around the hole observed in energy filtered images. The very straight holes are consistent with a high current density threshold for drilling, so that only the central portion of the beam etches, irrespective of its breadth.

A number of different mechanisms exist for electron stimulated desorption, and Humphreys *et al* (1985) suggested that the Knotek-Feibelman (1979) mechanism might be the dominant mechanism in  $\beta$ -alumina. An energy level diagram for Al<sub>2</sub>O<sub>3</sub> is given schematically in fig. 1. Al<sub>2</sub>O<sub>3</sub> in all its crystalline forms is highly ionic, and to a good approximation consists of Al<sup>3+</sup> and O<sup>2-</sup> ions. The highest occupied level of the Al<sup>3+</sup> ion is the 2p level. If an incident electron ionises this level, the dominant decay mode is an inter-atomic process in which one O(2p) electron decays into the Al(2p) hole. Since the O(2p) level has higher energy than the Al(2p) level, the inter-atomic decay process releases energy which can be taken up by the emission of one or two Auger electrons from the O(2p) state. The net result is that the Al ion remains Al<sup>3+</sup>, but that the O<sup>2-</sup> ion can lose up to 3 electrons and become O<sup>+</sup>. It is then ejected from the surface by the repulsive Coulomb force.

The region of specimen under the centre of the incident electron beam will be positively charged due to ionisation. The region outside the beam will be negatively charged due to the accumulation of low energy secondary electrons in the material. There is therefore a very strong electric field inside the specimen, acting radially outwards from the centre of the irradiated area, and it is this field which is probably responsible for sweeping the cations (i.e. Al<sup>3+</sup> ions) out towards the edge of the irradiated area (see fig. 2). The material therefore drills atom plane by atom plane: oxygen ions are desorbed, Al<sup>3+</sup> ions are swept to the sides of the hole thus uncovering further oxygen which then desorbs, etc. One further point is worth noting concerning electric fields. In a partially drilled specimen, the electric field in the 'partial hole' is vertically up or down (see fig. 2). The O<sup>+</sup> ions are therefore desorbed from the surface and swept out of the hole, as required to form holes which have very large aspect ratios. If the oxygen were desorbed as neutral O or O<sup>-</sup> it is likely that it would be adsorbed on the walls of a hole and combine with the excess Al there. The evidence is therefore consistent with Knotek-Feibelman type desorption with the oxygen being desorbed as O<sup>+</sup>. Unfortunately the quantities of material involved are very small and it is difficult to verify this directly.

If the incident electron current density is just below the level for drilling a hole, the oxygen under the beam is desorbed but a plug of Al metal is left in the hole (Humphreys *et al*, 1985). For lower beam current densities there is no metallisation, oxygen is desorbed from surface layers only and then the process stops, with the aluminium rich surfaces preventing further desorption. It is suggested that at incident current densities below the threshold for etching a complete hole, the ionisation rate is reduced and the radial electric field gradient in the specimen falls below some critical value which is required to sweep the Al<sup>3+</sup> ions towards the sides of the hole before they neutralise their charge by attracting electrons to become neutral Al metal.

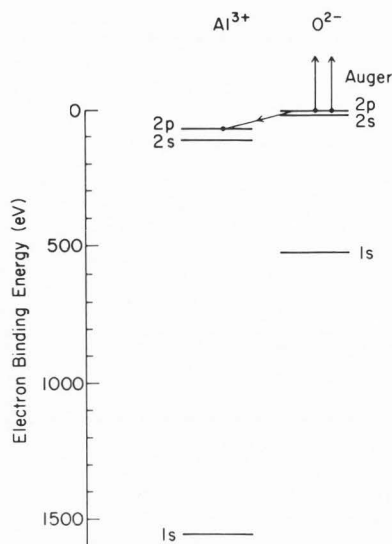


Figure 1 Schematic electron energy level diagram for  $\text{Al}_2\text{O}_3$ .

#### Nano-etching in amorphous alumina

Etching of a nanometre diameter hole in amorphous alumina ( $\alpha\text{-Al}_2\text{O}_3$ ) occurs in a very different way from that of the chemically similar crystalline  $\beta\text{-Al}_2\text{O}_3$ . The main similarity between the two processes is that in both materials the threshold current density for drilling a hole decreases with decreasing incident electron energy (i.e. it is easier to drill at lower energies) (Salisbury *et al.*, 1984) thus suggesting that for both materials ionisation damage is the primary mechanism responsible for electron beam etching.

Whereas etching a hole in  $\beta\text{-Al}_2\text{O}_3$  proceeds at a uniform rate, in  $\alpha\text{-Al}_2\text{O}_3$  the drilling is initially fast, then very slow, and lastly a hole is formed extremely rapidly. Fig. 3 shows the variation of the transmitted electron current as a function of time during the drilling of a hole (Berger *et al.*, 1987). The slowly rising plateau region occupies typically between 15s to 80s, and the final sharp rise in transmitted intensity occurs too rapidly to measure on our existing equipment.

If the incident electron beam is switched off before a complete hole has been formed in  $\beta\text{-Al}_2\text{O}_3$ , then the indentations at the top and bottom surfaces are unaltered when re-examined subsequently. On the other hand, if an incident beam on  $\alpha\text{-Al}_2\text{O}_3$  is switched off in the 'plateau' region of fig. 3, 'healing' occurs and no sign of an embryonic hole remains. Whereas EELS spectra using characteristic lines from  $\beta\text{-Al}_2\text{O}_3$  during drilling reveal a loss of oxygen from the irradiated volume, and an increase in the Al:O ratio, in  $\alpha\text{-Al}_2\text{O}_3$  the aluminium is lost and in the plateau region the material sampled is almost entirely oxygen, with an Al:O ratio of less than 0.1 (Berger *et al.*, 1987). Whereas the Al L edge disappears during drilling of  $\alpha\text{-Al}_2\text{O}_3$ , the oxygen K edge remains strong but changes dramatically with a sharp peak appearing at 532 eV, corresponding to molecular  $\text{O}_2$ . Although metallisation can occur in  $\beta\text{-Al}_2\text{O}_3$ , it is never observed in  $\alpha\text{-Al}_2\text{O}_3$ .

The above results are consistent with the following model which is a slight modification of that due to Berger *et al.* (1987). We suggest that the initial sharp increase in transmitted intensity (fig. 3) is due to the removal of aluminium from under the incident beam, accompanied by the formation of oxygen gas bubbles. Oxygen is also desorbed from the surfaces of the specimen to leave an Al surface capping layer which prevents further oxygen desorption. In

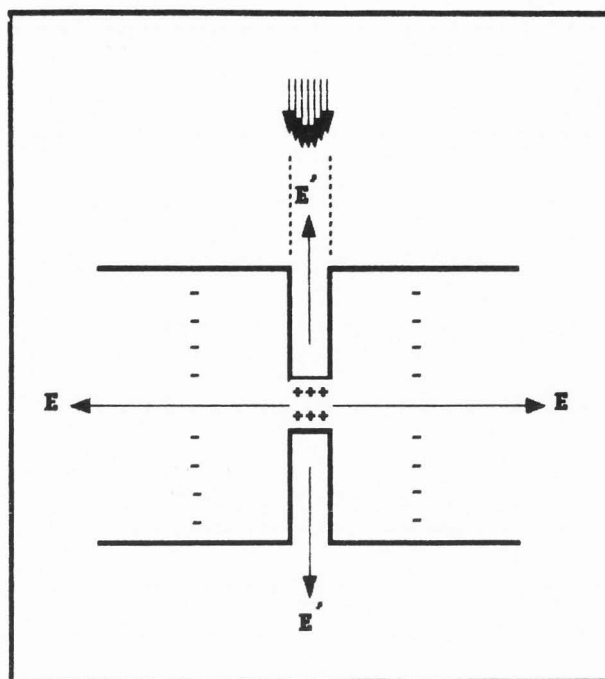


Figure 2 Schematic diagram of charge distribution and electric fields around a partially drilled hole in crystalline  $\beta$ -alumina.

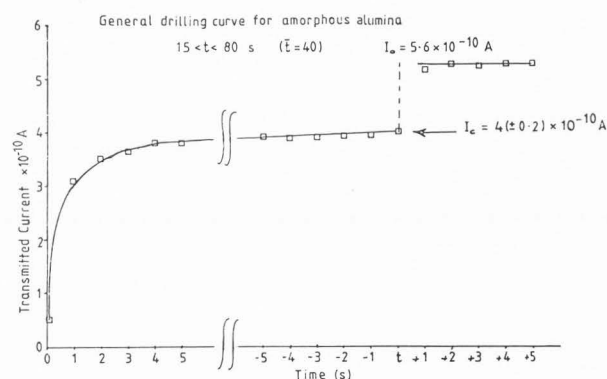


Figure 3 Variation of transmitted electron current as a function of time during the drilling of a hole in  $\alpha\text{-Al}_2\text{O}_3$ .

the plateau region of fig. 3 the oxygen bubbles slowly coalesce and eventually burst through the capping layer(s) leaving a hole. We have not yet determined whether both top and bottom capping layers are broken so that the hole is complete, or whether only one layer is broken through. If the beam is switched off in the plateau region of fig. 3, Al at the sides of the previously irradiated volume diffuses back in, recombines with the oxygen and the embryonic hole is healed. Considerable enhancement of the rate of etching of  $\alpha\text{-Al}_2\text{O}_3$  has been observed if the specimen is cooled to liquid nitrogen temperature (Devenish *et al.*, 1988 and 1989). This result is consistent with the back-diffusion of Al into the irradiated volume being reduced at low temperatures, hence the 'healing' is reduced and the hole production occurs more rapidly. The concept of an oxygen bubble bursting is consistent with the extremely sharp rise in the transmitted electron intensity at the



end of the etching process (fig. 3).

It is suggested that a Knotek-Feibelman type of mechanism may apply to the surface layers of  $\alpha\text{-Al}_2\text{O}_3$ , resulting in oxygen desorption from both surfaces. For structural reasons which are not yet clear a capping layer of Al forms in  $\alpha\text{-Al}_2\text{O}_3$  but not in crystalline  $\beta\text{-Al}_2\text{O}_3$  under intense electron irradiation. The reason for this may be due to different surface migration rates of Al ions in amorphous and crystalline  $\text{Al}_2\text{O}_3$ , and different charge distributions under the electron beam (Cazaux and Le Gressus, 1991).

Ionisation of both Al and O ions occurs in the bulk of the  $\alpha\text{-Al}_2\text{O}_3$ , due to Knotek-Feibelman and other mechanisms (some based on the early model due to Varley, 1962). The random network amorphous structure which was previously locally charge neutral is therefore disrupted, and under the influence of the intense radial electric field gradient positive Al ions move towards the periphery of the irradiated volume and negative and neutral oxygen ions are trapped in the irradiated volume where they coalesce to form oxygen gas bubbles. Energy filtered images of holes formed in  $\alpha\text{-Al}_2\text{O}_3$  using electrons which have lost 15 eV, corresponding to the Al plasmon loss, demonstrate the presence of metallic Al around the periphery of the holes (Berger *et al.*, 1987).

The above model is consistent with the observation that the current-density threshold for etching a hole in  $\alpha\text{-Al}_2\text{O}_3$  is several orders of magnitude greater than that for  $\beta\text{-Al}_2\text{O}_3$ . In  $\beta\text{-Al}_2\text{O}_3$  the drilling process involves surface desorption of oxygen and surface migration of aluminium. In  $\alpha\text{-Al}_2\text{O}_3$ , on the other hand, the process involves bulk migration of aluminium and oxygen. It is well known that the activation energy for bulk diffusion is much greater than for surface diffusion. Hence the induced electric fields required to remove the aluminium ions in the bulk are greater, which requires a higher incident beam current density. Our model is therefore self-consistent.

#### Nano-etching in MgO crystals

Nanometre scale square holes and lines can also be etched in MgO crystals by the focused electron beam in the STEM (Devenish *et al.*, 1988, 1989 and Turner *et al.*, submitted for publication). The crystals are formed by burning magnesium turnings in air and collecting the MgO cubes on a holey carbon film. In cubes of dimensions less than about 100 nm, aligned to within a few degrees of  $\langle 100 \rangle$ , the focused electron beam initially creates small indentations about 1 nm in depth and with diameters similar to the beam diameter at both the electron entrance and exit surfaces. The exit surface indentation then grows back through the crystal until it meets the very slowly growing entrance surface indentation. The drilling rate is approximately 1 nm per second for a beam current density of  $10^8 \text{ Am}^{-2}$ , defined in terms of total probe current and a 2 nm FWHM probe size. Figure 4 shows a number of partially and fully drilled holes in an MgO cube tilted (after drilling) by about 10 degrees so as to reveal the hole profiles. Each hole is bounded by  $\{100\}$  faces (see fig. 5 (a)), the holes widening out from the entrance to the exit surface in a number of steps (see fig. 5 (b),(c)), some of which have been observed to be as small as one unit cell (0.42 nm). Holes can be produced in MgO at energies as low as 40 keV, although in contrast with  $\alpha$ -alumina and  $\beta$ -alumina no threshold current density for drilling has been found. X-ray analysis indicates that the Mg:O ratio under the beam remains constant throughout the hole drilling process.

The formation of holes in MgO using 100 keV electrons is surprising since neither bulk displacement damage nor radiolysis would seem to be possible. Bulk displacement damage is not possible at 100 keV since the threshold for knock-on bulk displacement damage by electrons was measured by Youngman *et al.* (1980) to be 460 keV at 300K.

Figure 4 Holes partially and fully drilled in an MgO cube orientated close to  $\langle 001 \rangle$  and then tilted through  $10^\circ$  about a vertical axis. For each hole the electron exit surface is towards the left-hand side. Holes labelled (a), (b) and (c) have been drilled for 30s, 60s and 90s respectively under otherwise identical conditions.

Figure 5 Holes drilled in an MgO cube close to  $\langle 001 \rangle$ . (a) Square holes viewed down  $\langle 001 \rangle$ . (b) The same holes tilted  $10^\circ$  about a vertical axis, the electron exit surface towards the right-hand side for each hole. (c) Part of the same crystal tilted  $10^\circ$  about a horizontal axis, the electron exit surface towards the top of the image for each hole.

Figure 6 Five rows of voids formed in 160 nm  $\langle 001 \rangle$  Al along the irradiated volume for exposure times of 5, 4, 3, 2 and 1 minutes, viewed after tilting  $30^\circ$  about a horizontal axis; the electron entrance (exit) surface is towards the top (bottom) of the image.

Figure 7 Two holes formed in  $\langle 001 \rangle$  Si, each about 1.5 nm diameter and 60-90 nm long, viewed after tilting  $20^\circ$  about a horizontal axis; the electron entrance (exit) surface is towards the top (bottom) of the image.

Bulk radiolysis in MgO cannot occur by an exciton decay process (Kabler and Williams, 1978; Hobbs 1990) because the displacement energy for the ions is greater than the available energy of the exciton. Since radiolysis has never been observed in MgO (Reimer 1989), it would seem that the desorption of oxygen following multiple ionisation, by a Knotek-Feibelman or other mechanism, cannot occur. Presumably this is because the lifetime of a multiple hole state on an oxygen ion is less than the time required to desorb the ion. Since it appears that radiolysis and bulk displacement damage can both be ruled out, different mechanisms for mass loss must be operating in MgO. As noted above, windowless X-ray spectra show no build up of Mg or of O around the hole in an MgO crystal. In addition, material removed from the crystal by electron irradiation was collected on a carbon film, and windowless X-ray analysis showed this to be stoichiometric MgO. It is concluded that under electron irradiation, MgO molecules and/or clusters are desorbed (there is both experimental (e.g. Lagerquist and Uhler, 1949) and theoretical (e.g. Thummel *et al.*, 1989) evidence that MgO can exist in molecular form). Mass removal primarily from the electron exit surface suggests that this is assisted by momentum transfer from the electron beam.

The mechanism proposed for hole formation in MgO involves the creation of vacancy pairs in the (001) facet normal to the electron beam direction at the hole tip. This is thought to be the rate determining step. The resultant neutral MgO molecule moves to adjacent hole walls by rapid surface diffusion. Subsequent enlarging of the hole at the tip takes place by the creation of further vacancy pairs either in the (001) facet or at edge/corner sites. MgO molecules so removed will diffuse rapidly along the inner faces of the hole and in the direction of the electron exit surface, being evaporated from a suitable step by a momentum assisted process.

#### Nano-etching in Al and Si

The bulk displacement energy in aluminium (16-19 eV) is considerably greater than the maximum recoil energy transfer from 100 keV electrons in direct elastic collisions (9.2 eV). However, bulk displacement damage and hole formation have been found to occur in Al using the focused electron beam in the STEM (Bullough *et al.*, 1990a,b). Figure 6 shows the evolution of rows of voids formed along the

Fig. 4

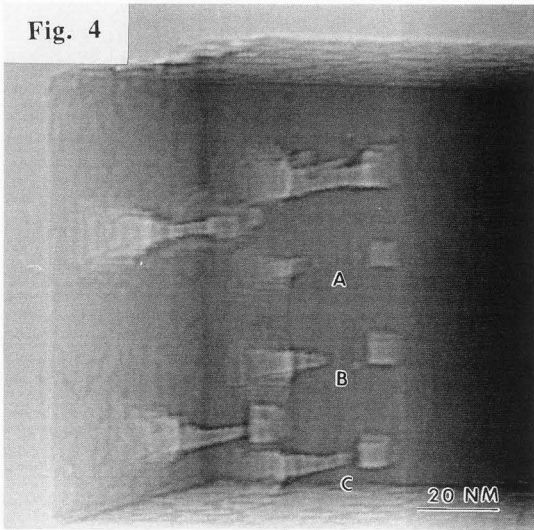


Fig. 5A

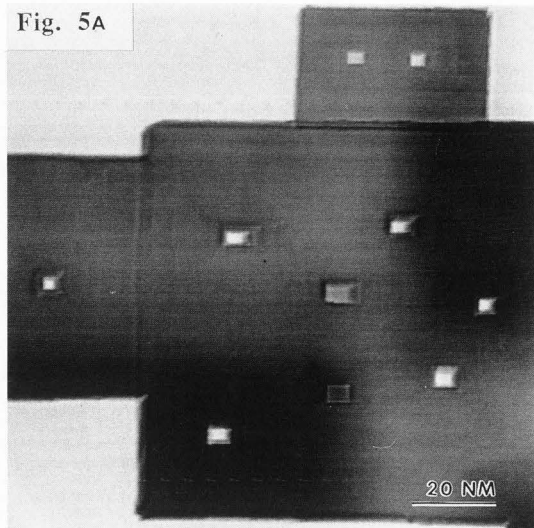


Fig. 6

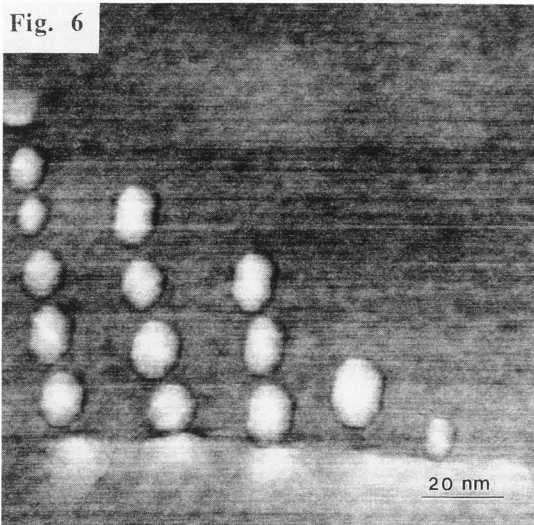


Fig. 5B

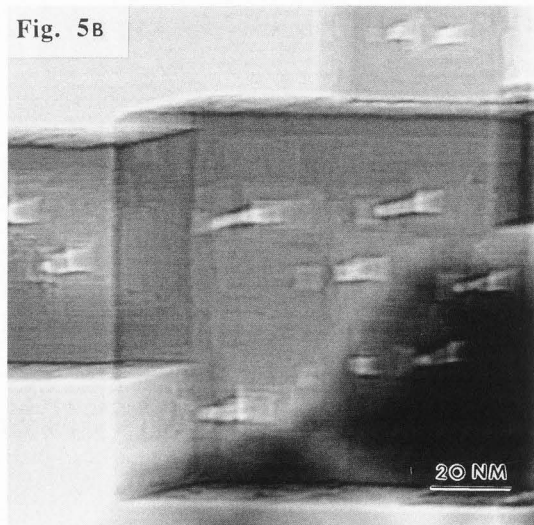


Fig. 7

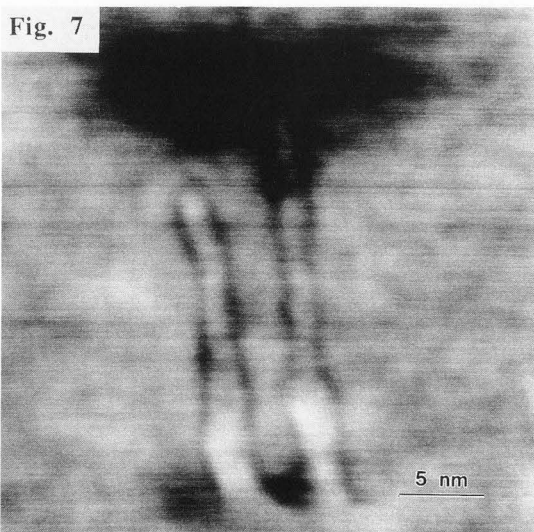
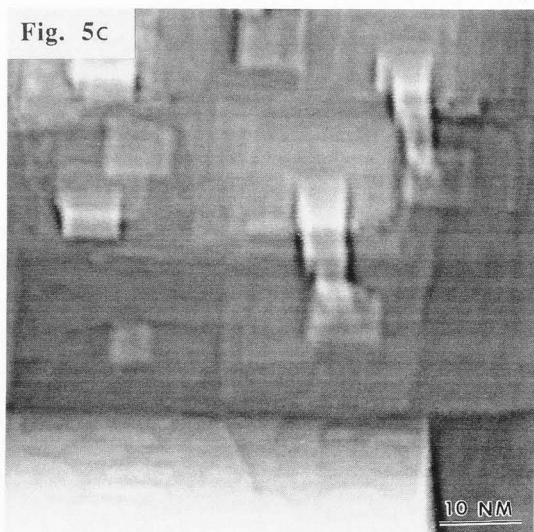


Fig. 5c



irradiated volume in a 160 nm thick <001> Al specimen by the stationary focused electron probe in the STEM. The 5 rows of voids seen in the figure, formed after irradiation times of 5, 4, 3, 2 and 1 minute respectively, have been subsequently tilted through 30° after formation, to reveal their profiles. Initial void growth is at the electron exit surface, with voids forming nearer to the electron entrance surface after exposure times of more than two minutes. The voids are typically 3-5 nm in diameter and can sometimes grow up to 35 nm in length. After prolonged irradiation a pit is formed at the electron entrance surface, which grows inwards and eventually forms a complete hole through the crystal.

The mechanisms responsible for this nano-etching in Al are not fully understood at present. The presence of light impurity elements, such as hydrogen, can raise the energy transfer to a lattice atom above the bulk displacement energy via a two-stage process, involving first electron-hydrogen atom and then hydrogen atom-aluminium atom elastic collisions (Bond *et al.* 1987). It is not yet clear how the point defects generated would then aggregate into the final damage structures seen within the irradiated volume. X-ray spectra acquired during void growth and hole formation show that the initial very low level (3-5%) of oxygen present as a thin residual oxide film on the Al surface is reduced to levels below the detection limit (<1%) within 10 seconds of exposure to the electron probe. There is no evidence from EELS spectra of large amounts of oxygen or hydrogen being present in the voids formed in the present study.

As well as unexpected displacement damage being produced in Al, the focused electron beam in the STEM can create bulk damage in Si. In Si the bulk displacement energy (11-22 eV) is also much greater than the maximum transferable recoil energy from 100 keV electrons in elastic collisions (8.8 eV). Figure 7 shows two partial holes, each formed by exposure of a 100 nm <001> Si specimen to the stationary electron probe for 60 seconds. The holes have been tilted by 20° to reveal their profiles. They have diameters of about 1.5 nm and have grown inwards from the electron exit surface at a rate of 1.0-1.5 nm/sec for an electron probe current density of  $2 \times 10^8 \text{ Am}^{-2}$ .

#### Nanolithography and information storage

Richard Feynman (1960), in a paper entitled "There's Plenty of Room at the Bottom", posed the question "Why cannot we write the entire 24 volumes of the Encyclopaedia Britannica on the head of a pin?" He proposed that the electron microscope was the instrument to do this, but that in 1959 "it was not quite good enough". Fig. 8 demonstrates that the contents of the Encyclopaedia Britannica can indeed be written on a pinhead using an electron microscope. The writing is a portion of the Encyclopaedia and each dot is a hole 4 nm in diameter drilled through  $\text{AlF}_3$ . As shown earlier, it is possible to form holes less than 1 nm in diameter. At this size, not only will the entire contents of the 24 volumes of the Encyclopaedia that existed in 1959 fit on a pinhead, but so will the contents of the 29 volumes of today's Encyclopaedia Britannica. If the letters are represented by a code of dots and dashes then the contents of the Encyclopaedia fit on a pinhead with plenty of room to spare.

The above nano-lithography demonstrates the potential of nanometre-scale electron probes for information storage, the fabrication of nanometre-scale three-dimensional electronic devices, tailor-made molecular sieves and microporous filters, catalysts, very high density memories, etc. Electron-beam nano-etching occurs in a wide range of materials, it involves some fascinating science, and it is likely to become an increasingly important area as the demand for miniaturisation and nanotechnology extends across a broad range of industries.

#### Acknowledgements

The authors are grateful to the Science and Engineering Research Council for support.

#### References

- Berger SD, Salisbury IG, Milne RH, Imeson D, Humphreys CJ. (1987). Electron energy-loss spectroscopy studies of nanometre-scale structures in alumina produced by intense electron-beam irradiation. *Phil. Mag.* **B55**, 341-358.
- Bond GM, Robertson IM, Zeides FM, Birnbaum HK. (1987). Sub-threshold electron irradiation damage in hydrogen-charged aluminium. *Phil. Mag.* **A55**, 669-681.
- Broers AN, Cuomo JJ, Harper J, Molzen M, Laibowitz R, Pomerantz M. (1978). High resolution electron beam fabrication using STEM, in: *Electron Microscopy 1978*, J.M. Sturgess (ed), Microscopical Society of Canada, Toronto, **3**, 343-354.
- Bullough TJ, Devenish RW, Humphreys CJ. (1990a). 100 keV electron-beam modification of aluminium and silicon in the STEM, in: *Electron Microscopy and Analysis 1989*, Inst. Phys. Conf. Ser., P.J. Goodhew (ed), Adam Hilger, London, in press.
- Bullough TJ, Humphreys CJ, Devenish RW. (1990b). Electron-beam induced nanometre hole formation and surface modification in Al, Si and MgO, in: *Materials Research Society Symposia Proceedings*, Materials Research Society, Pittsburgh, in press.
- Cazaux J, Le Gressus C. (1991). Phenomena related to charge in insulators: macroscopic effects and microscopic causes, in: *Scanning Microscopy* (to be published).
- Devenish RW, Eaglesham DJ, Maher DM, Humphreys CJ. (1988). Nanometre scale lithography in the CTEM, in: *EUREM 88: Proc. 9th European Congress on Electron Microscopy*, P.J. Goodhew and H.G. Dickinson (ed), Institute of Physics Conference Series 93, Institute of Physics, Bristol and Philadelphia, **2**, 391-392.
- Devenish RW, Eaglesham DJ, Maher DM, Humphreys CJ. (1989). Nanolithography using field emission and conventional thermionic electron sources. *Ultramicroscopy* **28**, 324-329.
- Feynman RP. (1960). There's plenty of room at the bottom, in: *Miniaturisation*, H.D. Gilbert (ed), Chapman and Hall, London and New York, 282-296.
- Hobbs LW. (1990). Murphy's Law and the uncertainty of electron probes, in: *Scanning Microscopy Supplement 4*, 1990,
- Humphreys CJ, Salisbury AG, Berger SD, Timsit RS, Mochel ME. (1985). Nanometre-scale electron beam lithography, in: *Electron Microscopy and Analysis 1985*, Inst. Phys. Conf. Ser.78, G.J. Tatlock (ed), Adam Hilger, London, 1-6.
- Isaacson M, Muray AJ. (1981). In-situ vaporisation of very low molecular weight resists using 0.5 nm diameter electron beams. *J. Vac. Sci. Technol.* **19**, 1117-1120.
- Kabler MN, Williams RT. (1978). Vacancy-interstitial pair production via electron-hole recombination in halide crystals. *Phys. Rev. B* **18**, 1948-1960.
- Knotek ML, Feibelman PJ. (1979). Stability of ionically bonded surfaces in ionising environments. *Surface Science* **90**, 78-90.
- Lagerquist A, Uhler U. (1949). The red and green bands of magnesium oxide. *Arkiv för Fysik* **1**, 459-475.
- Mochel ME, Humphreys CJ, Eades JA, Mochel JM, Petford AK. (1983). Electron beam writing on a 20Å scale in metal  $\beta$ -aluminas. *Appl. Phys. Lett.* **42**, 392-394.
- Mochel ME, Humphreys CJ, Mochel JM, Eades JA. (1983b). Cutting of 20Å holes and lines in metal  $\beta$ -aluminas,



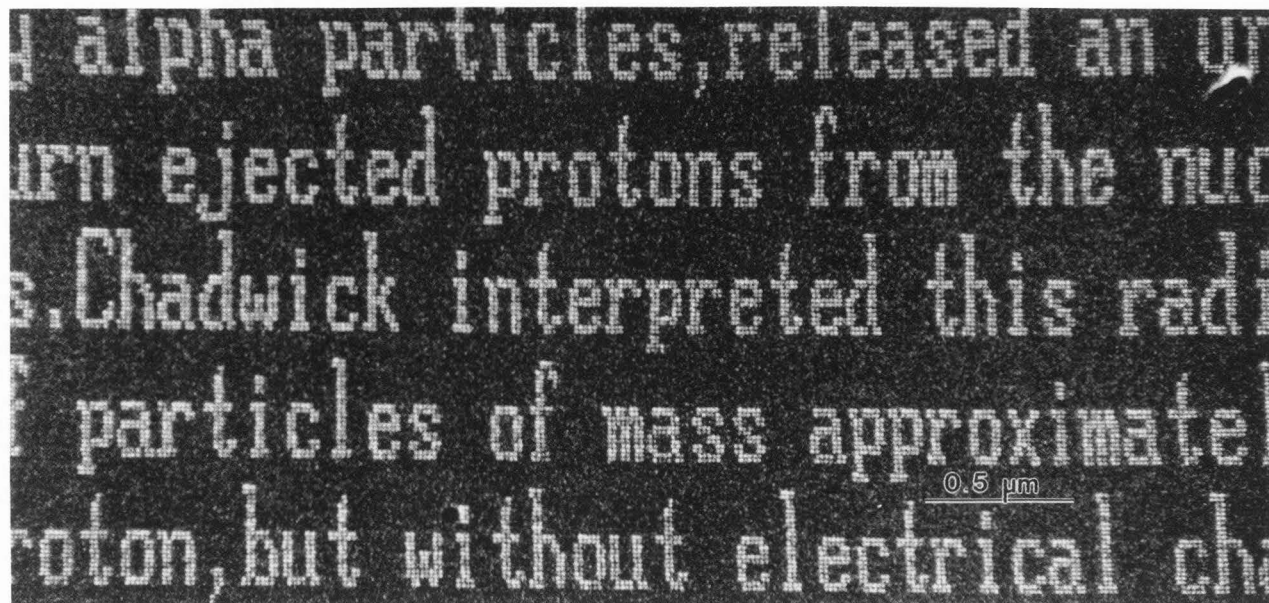


Figure 8 Encyclopaedia Britannica on a pinhead. The figure shows a portion of the Encyclopaedia written in  $\text{AlF}_3$ . Each hole is 4 nm in diameter. The figure reproduces a part of page 706 of Encyclopaedia Britannica referring to Chadwick (Micropaedia, Vol. II, Bibai to Coleman. 15th edition, Helen Hemingway Benton: Chicago and London, 1979).

in: Proc. 41st Annual Meeting of the Electron Microscopy Society of America, G.W. Bailey (ed), San Francisco Press, San Francisco, 100-101.

Reimer L. (1989). Transmission Electron Microscopy, Springer-Verlag, Berlin and New York, 453-457.

Salisbury IG, Timsit RS, Berger SD, Humphreys CJ. (1984). Nanometre scale electron beam lithography in inorganic materials. *Appl. Phys. Lett.* **45**, 1289-1291.

Thummel H, Klotz R, Peyerimhoft SD. (1989). The electronic structure of the MgO molecule in ground and excited states. *Chem. Phys.* **129**, 417-430.

Varley JHO. (1962). Discussion of some mechanisms of F centre formation in alkali halides. *J. Phys. Chem. Solids*, **23**, 985-1005.

Youngman RA, Hobbs LN, Mitchell TE. (1980). Radiation damage in oxides, electron irradiation damage in MgO. *J. de Phys.* **41**, C6, 227-231.

#### DISCUSSION WITH REVIEWERS

**W. Heiland:** The Knotek-Feibelman mechanism is independent of current or current density of the incident electrons. Yet you observe a current density threshold!

**Authors:** The Knotek-Feibelman mechanism concerns desorption of the anion and this is indeed independent of current or current density. However, to form a hole cations must also be removed, and it is this process which has been reported to have a current density threshold. However, as reported in this paper, there is no current density threshold in MgO. Also our recent work on  $\text{AlF}_3$  (unpublished) indicates that there is no current density threshold in this material. This interesting question is yet to be fully resolved.

**P. Nordlander:** Is there a limit to the thickness you can drill by this method?

**Authors:** We have demonstrated that we can drill through a layer of  $\text{Al}_2\text{O}_3$  on a bulk substrate of Al (Salisbury *et al*, 1984). We believe we could form holes through bulk samples of many materials given sufficient time (but probably not in MgO and other materials in which electron beam etching occurs mainly from the electron exit surface).

**D. Newbury:** Could the shallow entrance hole in MgO be a result of the momentum transfer in the collision cascade caused by the entering beam electrons? The knock-on effect, even if minor, eventually may produce a component of momentum perpendicular to the surface, resulting in emission of atoms or molecules at the surface. Alternatively, could fast secondary electrons, which propagate laterally, cause the surface entrance hole?

**Authors:** The mechanism for producing the shallow entrance hole is not yet clear. Fast secondary electrons or backscattered primary electrons are possible candidates for transferring momentum to entrance surface molecules.

**K. Krishnan:** I am surprised that you could interpret your concentration of oxygen/Mg (i.e. there is no change in stoichiometry) so accurately. My understanding is that there is about 15-20% error in the cross-sections that are used. Additionally there are substantial thickness variations occurring in the process that also need to be considered in such microanalysis.

**Authors:** We measured relative changes in the Mg:O ratio using windowless EDX. It was clear from our results that the Mg:O ratio stays constant during hole formation, showing that there is no excess Mg or O produced in this process. This situation is very different from, for example,  $\text{Al}_2\text{O}_3$ ,  $\text{AlF}_3$  or ZnO, in which both EELS and windowless EDX show that the material left around the holes after hole formation is non-stoichiometric.

**H. Kohl:** You drilled your holes in MgO using a  $\langle 100 \rangle$  orientation. What influence on beam spreading would you expect from the channelling effect?

**Authors:** The beam spreading due to elastic scattering in a  $\langle 100 \rangle$  orientation is less than that in an arbitrary orientation because the direction of electron energy flow is normal to the



dispersion surface branches at the wave points, and the dispersion surface branches are flat at  $\langle 100 \rangle$  orientation. The beam spreading due to inelastic scattering, in particular due to phonon scattering, will also be affected by the channelling effect.

K. Krishnan: Whilst I agree with your interpretations of the mechanisms underlying the nano-etching process, it would be very beneficial to know some additional details regarding the probe that was used. Have you characterised the probe shape, the current density in the probe, the tailing, i.e. FWHM, FWTM etc? If so, could you comment on the details.

Authors: We have measured the probe shape by scanning the beam across the face of an MgO cube and measuring the rise in the ADF signal. Typically we use 1 nA in a beam of 2.5 nm FWHM at 100 kV. At 40 kV the probe is also 2.5 nm FWHM but with lower current. The detailed shape of the probe is very sensitive to microscope alignment, etc. The smallest probes are non-Gaussian. The central portion is narrower than a Gaussian, and the tails are more extended. Smaller probes than 2.5 nm are possible by increasing the C2 lens excitation, and we use these when required.

J. Cazaux: The differences of experimental effects observed on  $\beta$ -alumina and amorphous alumina may be explained by the fact that the trapped charge distributions and thus the field they create are different. In amorphous alumina, the trapping defects are expected to be homogeneous in the specimen leading to a positive charge density,  $\rho_a$ , homogeneous inside a cylinder of radius  $a$  (beam radius) and height  $t$  (thickness of the specimen). In the single crystal, the charges may only be trapped on the surface defects. The field thus created is that of two discs (neglecting the image effects) of radius " $a$ ", having a surface charge density  $\sigma_s$ . The radial field created by these two discs in the mid-plane leads to a maximum value in this plane far weaker than in the amorphous case. The general ideas giving rise to this particular analysis can be found in the paper of Cazaux and Le Gressus, this volume, and in the Cazaux 1986a and 1986b references cited in that paper.

Authors: We agree that electric field distributions may be very important in the electron beam nano-etching process and the analysis of Cazaux and Le Gressus is most interesting.

L.W. Hobbs: The authors don't indicate whether their ceramic specimens are coated or uncoated (so I presume they are uncoated), nor if they are monolithic ion-thinned foils or sherds. If the samples are monolithic, uncoated insulating foils, it is surprising that it is possible to position the electron probe with any accuracy, or indeed at all, given that the external electrostatic field generated should deflect the incoming electron beam.

Authors: All specimens were uncoated. Sodium  $\beta$ -alumina specimens were crushed from large polycrystals; amorphous alumina specimens were evaporated and were also produced by anodising Al and then dissolving the Al substrate; MgO cubes were produced by burning Mg in air; some of the Al and Si specimens were chemically thinned and some ion-beam thinned. The small electron probe, typically 1 nm across, was substantially smaller than the specimens used and it was normally extremely stable when placed on a ceramic specimen, presumably because the charging produced by the axially symmetric electron beam was itself symmetric with respect to the beam. It was only when the beam approached the edge of a ceramic specimen that it was deflected by the charging, necessarily asymmetric near an edge.

L.W. Hobbs: Have any nano-etching experiments been attempted on specimens with thin conductive coatings evaporated on one or both sides? Altering the nature of the electrostatic field should prove informative, given that the authors consider its effect to be instrumental in many of the removal mechanisms.

Authors: We have coated amorphous  $\text{AlF}_3$  with carbon and performed nano-etching experiments. It was possible to form holes in  $\text{AlF}_3$  with C coatings. Amorphous  $\text{AlF}_3$  behaves similarly to amorphous  $\text{Al}_2\text{O}_3$  under electron irradiation in that F gas bubbles (instead of O gas bubbles) form in the irradiated area, coalesce and then burst through the capping layer leaving a hole. Al moves to the side of the irradiated volume, and even with coated specimens we believe this may be due to the internal electric field (produced by charging following ionisation) which sweeps  $\text{Al}^{3+}$  ions out of the irradiated volume. Coating the specimen surfaces will result in these being at zero potential (if the coating is earthed), but the interior of an insulating specimen such as  $\text{AlF}_3$  can still maintain an electrostatic field which would be radial if both surfaces were coated.